Hole filling and interlayer coupling in $Bi_2Sr_2Ca_{1-x}Pr_xCu_2O_y$ single crystals

X. F. Sun, X. Zhao, and X.-G. Li
Department of Materials Science and Engineering, University of Science and Technology of China, Hefei 230026, China and Institute of Solid State Physics, Academia Sinica, Hefei 230031, China

H. C. Ku
Department of Physics, National Tsing Hua University, Hsinchu, Taiwan 300, China

(Received 5 October 1998)

Effects of Pr doping on the superconductivity and CuO_2 interlayer coupling of the Bi2212 system were studied carefully for $Bi_2Sr_2Ca_{1-x}Pr_xCu_2O_y$ ($x=0-0.78$) single crystals. T_c was suppressed gradually upon Pr substitution, which cannot be explained in Abrikosov-Gor'kov pair-breaking theory. Instead, the variations of T_c with Pr content, for both as-grown and air-annealed crystals, can be well described by a universal parabolic relation $T_c/T_{max}=1-82.6(n-0.16)^2$. The carrier concentration n was proved to decrease linearly with x, which confirms that hole filling is the main reason for T_c suppression. The superconducting volume faction also decreases with Pr content and is proportional to $1-\beta x^2$. This behavior was attributed to the loss of local superconductivity and weakening of CuO_2 interlayer coupling due to Pr substitution. The second peak in the magnetization curves of $Bi_2Sr_2Ca_{1-x}Pr_xCu_2O_y$ crystals B_{sp} was found to decrease with Pr content and is described by $B_{sp}=\Phi_0/(s\gamma)^2$ with the anisotropy factor $\gamma=\gamma_0/(1-Ax)$ in terms of the dimensional crossover from three-dimensional (3D) flux lines to 2D pancake vortices. The increase of γ with x further demonstrates the destruction of CuO_2 interlayer coupling by Pr substitution. [S0163-1829(99)02710-1]

I. INTRODUCTION

It is well known that the carrier concentration is the most important parameter of high-T_c superconductors, which determines both the normal state and superconducting state properties. For the 85 K superconductor $Bi_2Sr_2CaCu_2O_y$ (Bi2212), there have been extensive studies on the cationic substitution of Ca by the rare-earth (R) elements or Y (Refs. 1–14) to change the carrier density and to probe the underlying mechanism of superconductivity. Experiments have indicated that Y or rare-earth elements can substitute for Ca in Bi2212 and the doped structure does not change fundamentally, while a transition from superconductor to insulator occurs with progressive substitution of the rare-earth element. It was thought that hole filling rather than Abrikosov-Gor'kov pair-breaking mechanism is responsible for the T_c decrease in the R-doped Bi2212 system.[6,9,10] In this field, Pr substitution for Ca is an interesting problem, also because the mechanism of unusual T_c suppression due to Pr doping in the $R_{1-x}Pr_xBa_2Cu_3O_{7-\delta}$ system is still unclear.[15]

The interlayer coupling between CuO_2 layers in high-T_c materials is usually weak but plays a crucial role in the superconductivity and vortex dynamics.[16] $Bi_2Sr_2CaCu_2O_y$ is a representative highly anisotropic oxide with a very large anisotropic ratio γ of more than 100,[17,18] which means the CuO_2 interlayer coupling of Bi2212 is very weak. For its high anisotropy and weak interlayer coupling, Bi2212 single crystals show anomalous magnetization behavior between 20 and 40 K,[19–24] which is considered as a manifestation of the dimensional crossover from three-dimensional (3D) flux lines to 2D pancake vortices.[23,25] The position of the anomaly, or the so-called second peak, directly relates to anisotropy factor by $B_{2D}=\Phi_0/(s\gamma)^2$,[25] with Φ_0 being the flux quantum and s being the interspacing between CuO_2 bilayers. This provides a way to obtain γ of the Bi2212 system and so the degree of interlayer coupling. Previous results showed that oxygen content or I intercalation would decrease the anisotropy of Bi2212 single crystals,[26,27] i.e., strengthen the interlayer coupling. Since Ca is located in the center of the CuO_2 bilayer, the Pr substitution is expected to destroy the local superconductivity of CuO_2 block and so strongly affects the interlayer coupling. However, no direct experimental results can be found for the lack of Pr-doped Bi2212 single crystals.

For Pr-doped Bi2212 system, there have been some studies on the structure, resistivity, Hall effect, and magnetic susceptibility, but all were performed on the polycrystallinity samples.[6,7,9–12] To obtain the intrinsic physical properties of the Pr-doped Bi-2212 system, especially the Pr-doping effect on the CuO_2 interlayer coupling and anisotropy, study of a single crystal is necessary, which has been absent in the literature. Recently we have successfully grown $Bi_2Sr_2Ca_{1-x}Pr_xCu_2O_y$ single crystals from Bi-rich melts.[28] In this paper, we study Pr-doping effects on the superconductivity and the interlayer coupling of $Bi_2Sr_2Ca_{1-x}Pr_xCu_2O_y$ single crystals.

II. EXPERIMENT

$Bi_2Sr_2Ca_{1-x}Pr_xCu_2O_y$ single crystals were grown by a directional solidification method with the starting composition of $2.4Bi:2.0Sr:(1-x_s)Ca:(x_s)Pr:2.0Cu$, where the nominal Pr contents were $x_s=0-0.6$ and excess Bi_2O_3 was included to act as a flux for the crystal growth. Bi_2O_3, $SrCO_3$, $CaCO_3$, Pr_6O_{11}, and CuO (all purity $\geqslant 99\%$) were used as the raw materials. The actual Pr content of as-grown crystals were determined to be $x=0-0.78$ by energy-dispersive x-ray analysis using a scanning electron microscopy (Stereoscan 440, Leica). Details for crystal growth have been described elsewhere.[28] Pure-phase and high-oriented crystals with di-

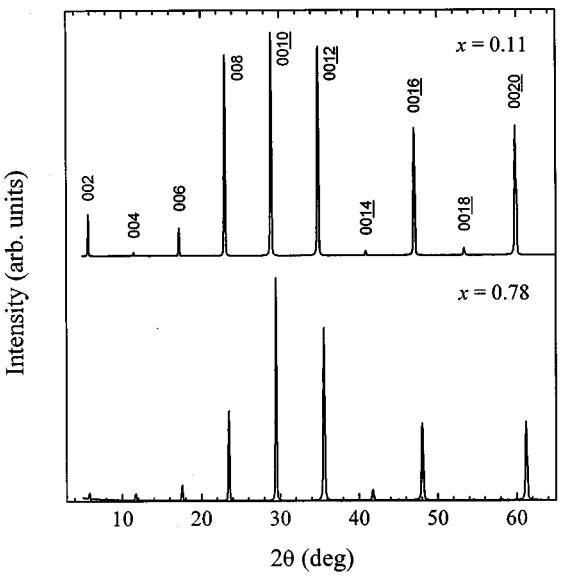

FIG. 1. Typical x-ray 00*l* diffraction of $Bi_2Sr_2Ca_{1-x}Pr_xCu_2O_y$ single crystals with $x=0.11$ and 0.78.

mensions around $3\times2\times0.03\ mm^3$ have been selected for the present work.

X-ray-diffraction data were collected using a rotating-anode diffractometer (Rigaku, $D/Max\text{-}\gamma A$) with graphite monochromatized Cu $K\alpha$ radiation. The dc magnetic susceptibility $\chi(T)$ and magnetization $M(H)$ measurements were carried out with a μ-metal-shielded Quantum Design $MPMS_2$ superconducting quantum interference device magnetometer down to 5 K in applied magnetic field from 1 G to 10 kG.

III. RESULTS AND DISCUSSIONS

Figure 1 shows the typical x-ray 00*l* diffraction patterns of $Bi_2Sr_2Ca_{1-x}Pr_xCu_2O_y$ single crystals for $x=0.11$ and 0.78. All the Pr-doped Bi2212 ($x=0-0.78$) single crystals have similar x-ray-diffraction patterns as those shown in Fig. 1, which indicates that the doped crystals possess the pure Bi2212 phase. The x-ray θ-scan rocking curves of main reflection 00$\underline{10}$ were also conducted to confirm that these crystals are highly oriented. Detailed characterizations on the structure of $Bi_2Sr_2Ca_{1-x}Pr_xCu_2O_y$ single crystals have been reported elsewhere.[29]

The variations of *c*-axis length with Pr content *x* for as-grown crystals are shown in Fig. 2. The *c*-axis length decreases monotonically with the increase of Pr content. Such a decrease in *c*-axis value may be due to one or more of the following reasons. First, the oxygen content in the system increases with Pr content for higher valence cation substitution. The decrease in *c*-axis length due to the increase of oxygen content has been reported for $Bi_2Sr_2CaCu_2O_y$ (Refs. 30–32) or rare-earth ion substitution at the Ca site.[9–11] Chen *et al.* had also reported the linear increase of oxygen and the linear decrease of the *c*-axis length with doping concentration for $Bi_2Sr_2Ca_{1-x}Pr_xCu_2O_y$ polycrystalline samples.[10] Second, there exist some Pr^{4+} ions in the system, the ionic size of which is smaller than that of Ca^{2+} ion. As far as the ionic sizes are concerned, the eightfold-coordinated ionic radii of Pr^{3+} and Pr^{4+} are 1.126 and 0.96 Å, respectively, while that of Ca^{2+} is 1.12 Å. Based on the large range of variation in the *c*-axis length, from 30.849 to 30.235 Å for $x=0$ to 0.78, it seems that the Pr exists in the Bi2212 phase between 3+ and 4+ valence states. Third, under Pr doping, an additional band crosses the Fermi level, grabbing holes from the CuO $pd\sigma$ band.[33] This attractive interaction, in fact, would result in the decrease of the separation between CuO_2 layers.

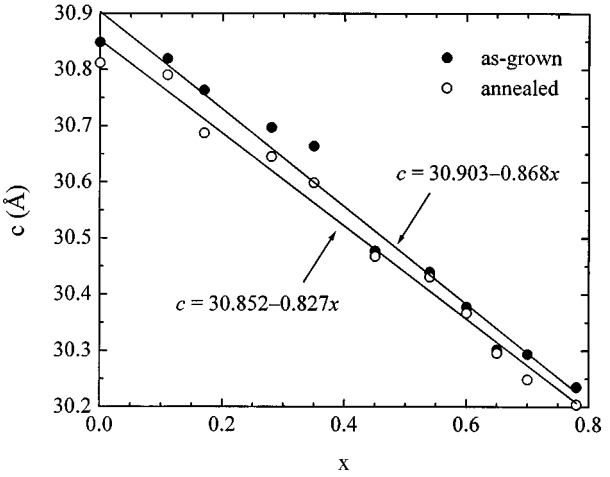

FIG. 2. Changes in the *c*-axis length with Pr content of $Bi_2Sr_2Ca_{1-x}Pr_xCu_2O_y$ single crystals as-grown and annealed in air at 360 °C. The lines are linear fits to the data.

All the selected crystals had been annealed in air at 360 °C for 60 h to improve the superconductivity. X-ray diffraction showed there is no phase decomposition in these air-annealed crystals, which is an outstanding characteristic for Bi2212 single crystals annealed at temperatures higher than 400 °C.[34,35] The changes of *c*-axis length with the Pr content for annealed crystals were also shown in Fig. 2. While the trend of *c*-axis variation is same for as-grown and annealed crystals, all the crystals shrink their *c*-axes after annealing in air at 360 °C. This is due to the increase of oxygen content after annealing crystals in air. In fact, the

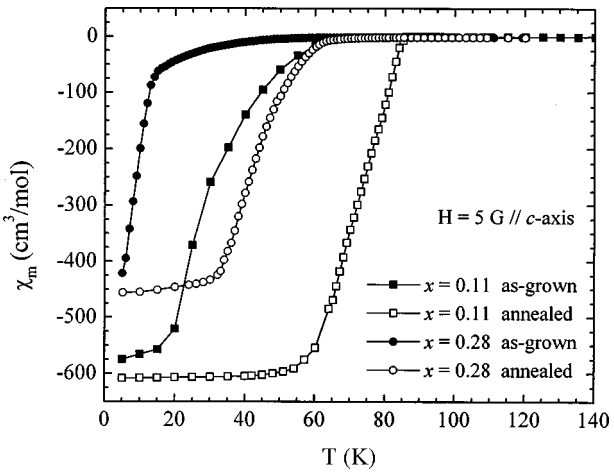

FIG. 3. Zero-field-cooled dc magnetic susceptibility $\chi_m(T)$ of $Bi_2Sr_2Ca_{1-x}Pr_xCu_2O_y$ ($x=0.11$ and 0.28) single crystals before and after air annealing at 360 °C. The measurements were carried out at a field of 5 G parallel to the *c* axis of each crystal.

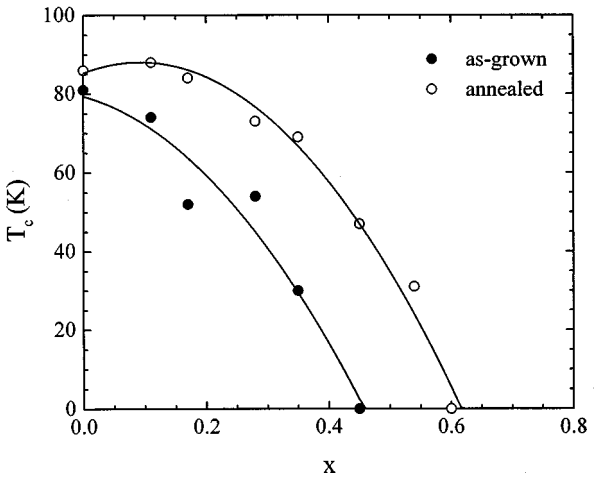

FIG. 4. Pr content dependence of superconducting transition temperature T_c for $Bi_2Sr_2Ca_{1-x}Pr_xCu_2O_y$ single crystals before and after air-annealing at 360 °C. The lines are the fitting to formula $T_c/T_{max}=1-82.6(ax+b)^2$ with parameters T_{max}, a, and b shown in Table I.

changes of c value with x can be well fitted linearly as

$$c=30.903-0.868x \quad (\text{Å}) \tag{1}$$

for as-grown crystals and

$$c=30.852-0.827x \quad (\text{Å}) \tag{2}$$

for annealed crystals, respectively. In these two relations, the smaller constant term of annealed crystals directly relates to the larger oxygen concentration. And the slower rate of c value decreasing with x for annealed crystals means that the oxygen contents are rich after annealing and constricts the additional increase of oxygen content due to the increase of Pr content.

Figure 3 shows the typical temperature dependence of the zero-field-cooled dc susceptibility for $Bi_2Sr_2Ca_{1-x}Pr_xCu_2O_y$ crystals measured at a field of 5 G parallel to the c axis. The superconducting transition temperature T_c can be determined as the onset transition of diamagnetic. Figure 4 gives the relation between T_c and the Pr content for crystals before and after annealing. The T_c of as-grown crystals are rather low and a little divergent, which were improved greatly after annealing the crystals in air. With the increase of Pr content for annealed crystals, T_c increases slightly at first, after reaching a maximum at $x=0.11$, and then drops gradually. Superconductivity is completely suppressed when the Pr content reaches 0.45 and 0.60 for crystals as-grown and air-annealed, respectively. This is reasonable because the oxygen content and so the carrier concentration is higher in annealed crystals than in as-grown ones. Next, we analyze the possible mechanism for T_c suppression induced by the Pr doping.

Abrikosov and Gor'kov[36] (AG) have pointed out that the presence of magnetic impurities in a superconductor breaks the time-reversal symmetry that causes a strong suppression of T_c. In the BCS limit, the reduced transition temperature (T_c/T_{c0}), in the presence of a paramagnetic impurity, is given by the relation

TABLE I. The fitting parameters T_{max}, a, and b for $Bi_2Sr_2Ca_{1-x}Pr_xCu_2O_y$ single crystals before and after annealing.

Parameter	As-grown	Annealed
T_{max} (K)	81	88
a	0.206	0.210
b	0.016	0.019

$$\ln(T_{c0}/T_c)=\Psi(1/2+\alpha)-\Psi(1/2), \tag{3}$$

where Ψ is the digamma function and α is the pair-breaking parameter. In AG theory, T_c decreases linearly with the concentration of magnetic ions (x) for small values of x, with a slope proportional to the magnitude of the exchange integral, a parameter characterizing the strength and sign of the exchange interaction between a paramagnetic impurity and a conduction electron. While at a large value of x, the decrease in T_c is more rapid. For present results, it is clear that the T_c suppression with x qualitatively deviates from the AG pair-breaking law, which means the magnetic nature of the Pr ions does not play an important role in the mechanism of T_c suppression. Previous results on Y or rare-earth doped Bi2212 polycrystalline samples also deny the application of the AG mechanism.[11] The alternative explanation may be the hole-filling effect due to the higher valence substitution of Pr ions for Ca ions.

As high-T_c superconductors are usually considered to be ionic, charges can be assigned to each of the constituent cations (metal ions) and anions (oxygen ions). Thus, for the Pr-doped Bi2212 system, the number of holes per copper atom would chemically be given as

$$n\approx n_1-0.5x, \tag{4}$$

where n_1 is a constant of the oxygen and strontium deficiency dependent. On the other hand, a well-known universal parabolic curve for describing the relation between T_c and carrier density n is[37,38]

$$T_c/T_{max}=1-82.6(n-0.16)^2. \tag{5}$$

This relation is valid for a wide class of high-T_c materials, regardless of the nature of the dopants. However, one cannot get a reasonable curve by combining Eqs. (4) and (5) to fit the present experimental data. Therefore, it is necessary to relate n to x from experimental results. Suppose n is proportional to x, then the relationship between T_c and x can be described as

$$T_c/T_{max}=1-82.6(ax+b)^2, \tag{6}$$

where a and b are constants. As shown in Fig. 4, Eq. (6) fits our experimental results well for both as-grown and annealed crystals. The fitting parameters are given in Table I. Combining Eqs. (5) and (6), we have

$$n=0.144-0.206x \tag{7}$$

for as-grown crystals and

$$n=0.179-0.210x \tag{8}$$

for annealed crystals, respectively. Comparing these two relations to Eq. (4), it can be seen that the CuO_2 layers in this

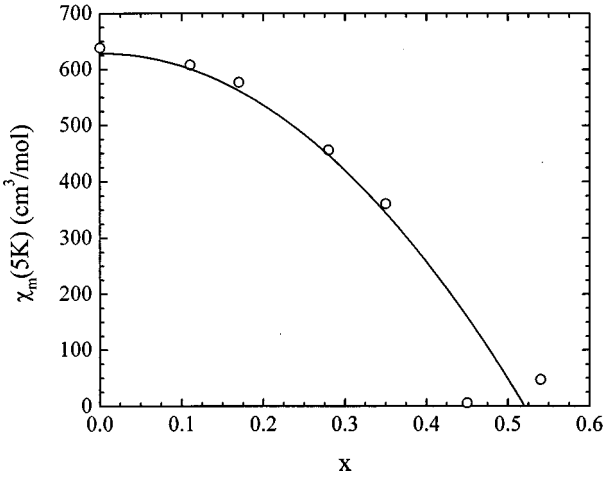

FIG. 5. Changes of the magnitude of the diamagnetic at 5 K with the Pr concentration for $Bi_2Sr_2Ca_{1-x}Pr_xCu_2O_y$ annealed crystals. The line is the fitting curve using $\chi_m(5\,\mathrm{K})=\chi_{m0}(1-\beta x^2)$ with parameters $\chi_{m0}=628.9\,\mathrm{cm}^3/\mathrm{mol}$ and $\beta=3.69$.

particular Pr doping benefit from less than half of the chemical doping. This may be due to the increase of oxygen content accompanied with Pr substitution. Anyway, Eqs. (7) and (8) indicate that the substitution of Pr for Ca in the $Bi_2Sr_2Ca_{1-x}Pr_xCu_2O_y$ system effectively reduces the hole concentration on CuO_2 layers to the underdoped state, i.e., the contribution to T_c suppression mainly comes from the hole-filling effect. Therefore, for the annealed crystals, the $x=0$ one is in the carrier overdoping region, the $x=0.11$ one is around the optimal doping, and the $x>0.11$ ones locate in the underdoping region. Moreover, the small difference between Eqs. (7) and (8) further confirms that the oxygen content increases for each crystal after annealing, which is consistent with the changes in *c*-axis length.

As shown in Fig. 3, the superconducting volume faction of $Bi_2Sr_2Ca_{1-x}Pr_xCu_2O_y$ single crystals also decreases with increasing Pr concentration. Figure 5 gives the changes of $\chi_m(5\,\mathrm{K})$, the magnitude of the diamagnetic at low temperature 5 K, with the Pr content for annealed crystals. The decrease of diamagnetic magnitude with x may relate to the destruction of CuO_2 interlayer coupling induced by substituting Pr for Ca. In the Pr-doped Bi2212 system, the local superconductivity is lost in the vicinity of randomly distributed Pr ions. Then effective superconducting area shrinks strongly due to Pr substitution, as shown in Fig. 6. The average superconducting area in one layer destroyed by a Pr ion is proportional to doping level x. Considering two CuO_2 layers above and below the Pr ion, the effective superconducting volume is expected to be proportional to $1-\beta x^2$, β is a proportional coefficient. Therefore, the $\chi_m(5\,\mathrm{K})$ can be described as

$$\chi_m(5\ \mathrm{K})=\chi_{m0}(1-\beta x^2), \tag{9}$$

where χ_{m0} is a constant. Equation (9) fits the experimental results well with the fitting parameters $\chi_{m0}=628.9\,\mathrm{cm}^3/\mathrm{mol}$ and $\beta=3.69$. Thus, the loss of local superconductivity in CuO_2 bilayers will dramatically weaken the interlayer coupling of the Bi2212 system.

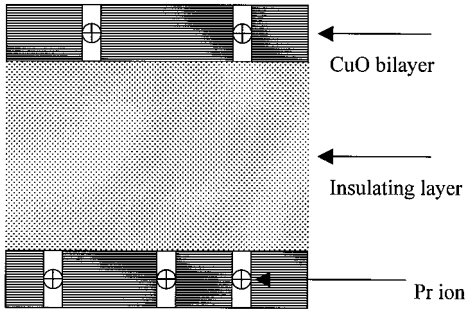

FIG. 6. Schematic illustration of the coupling between two adjacent CuO_2 bilayers in Pr-doped Bi2212. The region in the vicinity of Pr ions is normal-like due to the Pr substitution and the coupling between CuO_2 bilayers being weakened.

To further study the effect of Pr doping on the CuO_2 interlayer coupling of Bi2212, the second peak in magnetization curves were studied for annealed crystals. Figure 7 shows the typical temperature dependence of magnetization curves for $Bi_2Sr_2Ca_{1-x}Pr_xCu_2O_y$ ($x=0.17$) annealed crystals under a field parallel to the *c* axis. After the crystal was zero-field cooled to an experimental temperature, the magnetization was measured with increasing field. A second peak in magnetization curve occurs at field $B_{sp}\approx 340\,\mathrm{G}$, which is nearly temperature dependent. This anomaly appears in the temperature regions of 20–35 K, 20–30 K, 17.5–25 K, and 15–17.5 K for crystals $x=0$, 0.11, 0.17, and 0.28, respectively. And no second peak can be observed for crystals with $x>0.28$. The second peak field B_{sp} increases weakly with decreasing temperature, which is consistent with previous reports on Bi2212 crystals,[19–24] but decreases dramatically with the increase of Pr content. Figure 8 shows the magnetization curves for $Bi_2Sr_2Ca_{1-x}Pr_xCu_2O_y$ annealed crystals at 20 K for $x=0$, 0.11, 0.17, and 17.5 K for $x=0.28$, which ensures that the reduced temperature T/T_c for each crystal is very close to each other. Although the superconductivity of these four crystals changes from overdoping to optimal dop-

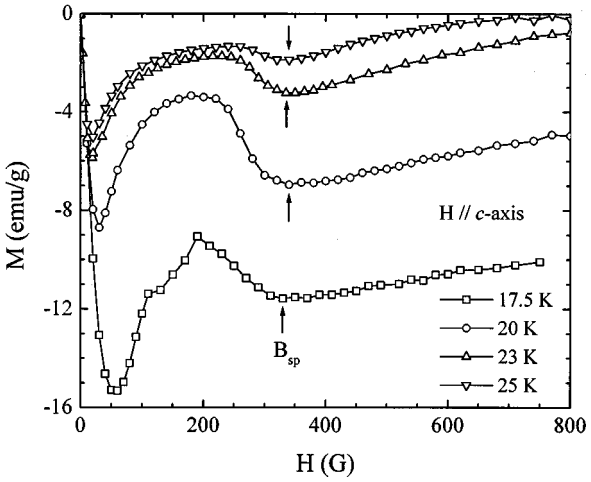

FIG. 7. Magnetization curves $M(H)$ for $Bi_2Sr_2Ca_{1-x}Pr_xCu_2O_y$ ($x=0.17$) annealed crystals at temperatures 17.5, 20, 23, and 25 K. The second peak B_{sp} for each curve was indicated by arrows.

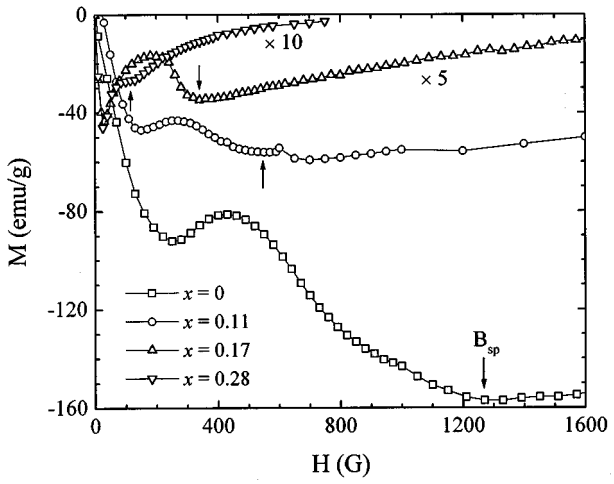

FIG. 8. Magnetization curves $M(H)$ for $Bi_2Sr_2Ca_{1-x}Pr_xCu_2O_y$ annealed crystals at 20 K for $x=0$, 0.11, 0.17, and 17.5 K for $x=0.28$. The second peak B_{sp} for each crystal was indicated by arrows. The small discontinuity in the $M(H)$ curve for the $x=0.11$ crystal is an artificial result induced by the increase in the rate of field sweeping.

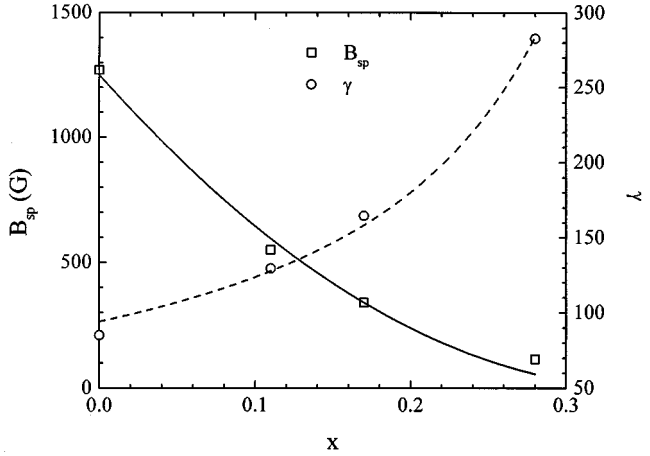

FIG. 9. Variations of the second peak B_{sp} and the anisotropy factor γ with the Pr content for $Bi_2Sr_2Ca_{1-x}Pr_xCu_2O_y$ annealed crystals. The solid line and dash line are fits to formula $B_{sp}=\Phi_0(1-Ax)^2/(s\gamma_0)^2$ and $\gamma=\gamma_0/(1-Ax)$, respectively.

ing and then to underdoping with increasing x, B_{sp} decreases monotonically with increase of the Pr content, as shown in Fig. 9.

As for the Bi2212 system, the origin of the second peak is generally explained as the dimensional crossover from 3D vortex lines to 2D pancake vortices, namely, decoupling of vortices in each CuO_2 bilayer. And the dimensional crossover field can be written as[25]

$$B_{2D}=\Phi_0/(s\gamma)^2, \tag{10}$$

where Φ_0 is the flux quantum, s is the interspacing between two CuO_2 blocks, and $\gamma=\lambda_c/\lambda_{ab}$ is the anisotropy parameter, where λ_{ab} and λ_c are the in-plane and out-of-plane superconducting penetration depths, respectively. From the relation between B_{2D} and γ, one can see that γ should increase with increasing Pr content. On the basis of the Josephson coupled block model and considering the loss of local superconductivity induced by ion substitution, Tang *et al.*[39] have found the relationship between the anisotropy parameter and the ion concentration substituted in $Y_{1-x}Pr_xBa_2Cu_3O_{7-\delta}$ system is

$$\gamma=\gamma_0/(1-Ax), \tag{11}$$

where γ_0 is a constant and A is a proportional coefficient. The Ca site in Bi2212 has an identical crystallographic environment to that of Y in Y123, both occupying the center of the Cu-O octahedra. So Eq. (11) should be also applicable for the Pr-doped Bi2212 system. Thus, the x dependence of the second peak field can be described as

$$B_{sp}=\frac{\Phi_0}{(s\gamma_0)^2}(1-Ax)^2. \tag{12}$$

Equation (12) fits the experimental data well, see the solid line in Fig. 9. Also shown in Fig. 9 are the changes of γ with x and fitting data to Eq. (11) with parameters $\gamma_0=94.0$ and $A=2.39$. These results demonstrate that the Pr doping surely weakens the CuO_2 interlayer coupling and increases the anisotropy of the Bi2212 system.

IV. CONCLUSIONS

Effect of Pr doping on the superconductivity and CuO_2 interlayer coupling of the Bi2212 system was studied carefully for $Bi_2Sr_2Ca_{1-x}Pr_xCu_2O_y$ ($x=0-0.78$) single crystals. The T_c variations with Pr content, for both as-grown and air-annealed crystals, can be well described by a universal parabolic relation $T_c/T_{max}=1-82.6(n-0.16)^2$. The carrier concentration n was proved to decrease linearly with x, which confirms that hole filling is the main reason for the suppression of T_c. The superconducting volume faction also decreases with Pr content and is proportional to $1-\beta x^2$, which was well described as the loss of local superconductivity of CuO_2 bilayers due to the Pr substitution. The second peak in magnetization curves, B_{sp}, was found to decrease with Pr content and described as $B_{sp}=\Phi_0/(s\gamma)^2$ and anisotropy factor $\gamma=\gamma_0/(1-Ax)$ in terms of the dimensional crossover from 3D flux lines to 2D pancake vortices. This result demonstrates the destruction of CuO_2 interlayer coupling by the Pr substitution, which relates to the loss of local superconductivity in each CuO_2 bilayer.

ACKNOWLEDGMENTS

This work was supported by the National Natural Science Foundation of China and the National Center for Research & Development on Superconductivity.

[1] J. M. Tarascon, P. Barboux, G. W. Hull, R. Ramesh, L. H. Greene, M. Grioud, M. S. Hedge, and W. R. McKinnon, Phys. Rev. B **39**, 4316 (1989).
[2] T. Tamegai, K. Koga, K. Suzuki, M. Ichihara, F. Sakai, and Y. Iye, Jpn. J. Appl. Phys., Part 2 **28**, L112 (1989).
[3] C. N. Rao, R. Nagarajan, R. Vijayraghavan, N. Y. Vasanthacharya, G. Kulkarni, G. Ranga Rao, A. M. Umarji, P. Somasundaram, G. N. Subbanna, A. R. Raju, A. K. Sood, and N. Chandrabhas, Supercond. Sci. Technol. **3**, 242 (1990).
[4] B. Jayaram, P. C. Lanchester, and M. T. Weller, Phys. Rev. B **43**, 5444 (1991).
[5] Y. Gao, P. Pernambuco-Wise, J. E. Crow, J. O'Reilly, N. Spencer, H. Chen, and R. E. Salomon, Phys. Rev. B **45**, 7436 (1992).
[6] C. Quitmann, D. Andrich, C. Jarchow, M. Fleuster, B. Beschoten, G. Güntherodt, V. V. Moshchalkov, G. Mante, and R. Manzke, Phys. Rev. B **46**, 11 813 (1992).
[7] C. Kendziora, L. Forro, D. Mandrus, J. Hartge, P. Stephens, L. Mihaly, R. Reeder, D. Moecher, M. Rivers, and S. Sutton, Phys. Rev. B **45**, 13 025 (1992).
[8] V. P. S. Awana, S. K. Agarwal, R. Ray, S. Gupta, and A. V. Narlikar, Physica C **191**, 43 (1992).
[9] V. P. S. Awana, S. K. Agarwal, A. V. Narlikar, and M. P. Das, Phys. Rev. B **48**, 1211 (1993).
[10] Xiaolong Chen, Jingkui Liang, Jinrong Min, Jianqi Li, and Guanghui Rao, Phys. Rev. B **50**, 3431 (1994).
[11] P. Sumana Prabhu, M. S. Ramachandra Rao, U. V. Varadaraju, and G. V. Subba Rao, Phys. Rev. B **50**, 6929 (1994).
[12] H. Jin, N. L. Wang, Y. Chong, M. Deng, L. Z. Cao, and Z. J. Chen, J. Cryst. Growth **149**, 269 (1995).
[13] V. P. S. Awana, Latika Menon, and S. K. Malik, Phys. Rev. B **51**, 9379 (1995); **53**, 2245 (1996).
[14] B. Beschoten, S. Sadewasser, G. Güntherodt, and C. Quitmann, Phys. Rev. Lett. **77**, 1837 (1996).
[15] Weiyan Guan, Yunhui Xu, S. R. Sheen, Y. C. Chen, J. Y. T. Wei, H. F. Lai, M. K. Wu, and J. C. Ho, Phys. Rev. B **49**, 15 993 (1994), and references therein.
[16] S. L. Cooper and K. E. Gray, in *Physical Properties of High Temperature Superconductivity IV*, edited by D. M. Ginsberg (World Scientific, Singapore, 1996), p. 61.
[17] R. Busch, G. Ries, H. Werthner, G. Kreiselmeyer, and G. Saemann-Ischenko, Phys. Rev. Lett. **69**, 522 (1992).
[18] J. C. Martinez, S. H. Brongersma, A. Koshelev, B. Ivlev, P. H. Kes, R. P. Griessen, D. G. De Groot, Z. Tarnavski, and A. A. Menovsky, Phys. Rev. Lett. **69**, 2276 (1992).
[19] V. N. Kopylov, A. E. Koshelev, I. F. Schegolev, and T. G. Togonidze, Physica C **170**, 291 (1990).
[20] N. Chikumoto, M. Konczykowski, N. Motohira, and A. P. Malozemoff, Phys. Rev. Lett. **69**, 1260 (1992).
[21] Y. Yeshurun, N. Bontemps, L. Burlachkov, and A. Kapitulnik, Phys. Rev. B **49**, 1548 (1993).
[22] K. Kadowaki and T. Mochiku, Physica C **195**, 127 (1992).
[23] T. Tamegai, Y. Iye, I. Oguro, and K. Kishio, Physica C **213**, 33 (1993).
[24] G. Yang, P. Shang, S. D. Sutton, J. P. Jones, J. S. Abell, and C. E. Gough, Phys. Rev. B **48**, 4054 (1993).
[25] V. M. Vinokur, P. H. Kes, and A. E. Koshelev, Physica C **168**, 29 (1990).
[26] Y. Kotaka, T. Kimura, H. Ikuta, J. Shimoyama, K. Kitazawa, K. Yamafuji, K. Kishio, and D. Pooke, Physica C **235-240**, 1529 (1994).
[27] D. H. Ha, K. W. Lee, K. Oka, Y. Yamaguchi, F. Iga, and Y. Nishihara, Physica C **260**, 242 (1996).
[28] Xuefeng Sun, Xia Zhao, Wenbin Wu, Xiaojuan Fan, and Xiao-Guang Li, Physica C **305**, 227 (1998).
[29] Xuefeng Sun, Xia Zhao, Wenbin Wu, Xiaojuan Fan, Xiao-Guang Li, and H. C. Ku, Physica C **307**, 67 (1998).
[30] H. W. Zandbergen, W. A. Groen, F. C. Mijlhoff, G. van Tendeloo, and S. Amelinckx, Physica C **156**, 325 (1989).
[31] G. Triscone, J. Y. Genoud, T. Graf, A. Junod, and J. Muller, Physica C **176**, 247 (1991).
[32] Xuefeng Sun, Wenbin Wu, Lei Zheng, Xiaoru Zhao, Lei Shi, Guien Zhou, Xiao-Guang Li, and Yuheng Zhang, J. Phys.: Condens. Matter **9**, 6391 (1997).
[33] A. I. Liechtenstein and I. I. Mazin, Phys. Rev. Lett. **74**, 1000 (1995).
[34] Wenbin Wu, Liangbin Wang, Xiao-Guang Li, Guien Zhou, Yitai Qian, Qiaonan Qin, and Yuheng Zhang, J. Appl. Phys. **74**, 7388 (1993).
[35] Wenbin Wu, Liangbin Wang, Qiaonan Qin, Yitai Qian, Lei Shi, Xiao-Guang Li, Guien Zhou, and Yuheng Zhang, Phys. Rev. B **49**, 1315 (1994).
[36] A. A. Abrikosov and L. P. Gor'kov, Zh. Eksp. Teor. Fiz. **39**, 1781 (1961) [Sov. Phys. JETP **12**, 1243 (1961)].
[37] M. R. Presland, J. L. Tollon, R. G. Buckley, R. S. Liu, and N. E. Flower, Physica C **176**, 95 (1991).
[38] S. D. Obertelli, J. R. Cooper, and J. L. Tallon, Phys. Rev. B **46**, 14 928 (1992).
[39] Hongxing Tang, Jinsheng Zhu, Xiao-Guang Li, and Yuheng Zhang, J. Appl. Phys. **79**, 1991 (1996).